DOI: https://doi.org/10.21323/2414-438X-2025-10-3-237-246
Received 22.05.2025
Accepted in revised 06.08.2025
Accepted for publication 19.08.2025
Available online at https://www.meatjournal.ru/jour
Original scientific article
Open Access

DEVELOPMENT OF A SPECTROPHOTOMETRIC APPROACH FOR ASSESSING PORK QUALITY DURING STORAGE

Viktar D. Raznichenka[1, 2],* Aleh U. Shkabrou[3], Lyubou U. Lazovikava[2]
[1] Slutsk Meat Processing Plant JSC, Slutsk, Republic of Belarus
[2] Belarusian State University of Food and Chemical Technologies, Mogilev, Republic of Belarus
[3] Ministry of Agriculture and Food of the Republic of Belarus, Minsk, Republic of Belarus

Keywords: *pork, meat quality control, spectrophotometry, extractants, absorption spectra*

Abstract
The annual growth of meat production, accompanied by significant quality deterioration at all stages of the production chain, drives the development of fast and highly accurate control methods. The work is devoted to the adaptation of the spectrophotometric method for assessing pork quality based on the analysis of muscle tissue extracts. The purpose of the work is to generalize and systematize knowledge about spectrophotometric analysis and the application of this method for pork quality control during storage. The work provides a comparative spectrophotometric assessment of various methods for extracting protein and non-protein components of pork muscle tissue. Aqueous, buffer, NaCl and KCl extracts of muscle tissue were studied, their absorption spectra in the wavelength range of 315–1000 nm were analyzed. It was found that KCl and NaCl extraction ensured the maximum degree of myofibrillar and sarcoplasmic protein extraction, and also formed the most pronounced and stable spectral peaks. Particular attention was paid to the analysis of KCl extracts demonstrating the best resolution and clarity of spectral curves, which is important for a detailed study of changes in muscle tissue properties during storage. During meat storage, statistically significant changes in the intensity and geometry of key spectral peaks ($\lambda_{325–335}$, λ_{355}, $\lambda_{410–415}$, λ_{545}, λ_{580}, $\lambda_{610–620}$, $\lambda_{635–650}$) were revealed, which were simultaneous with histostructural transformations of muscle tissue. A high correlation was established between the change in the area of minor peaks and the dynamics of muscle fiber diameter, which allows using spectral characteristics as objective indicators for the degree of changes in muscle tissue at the cellular and molecular levels during storage. The results obtained confirm the feasibility of using spectrophotometric analysis of KCl extracts for an objective assessment of meat quality and monitoring its changes at various stages of storage.

For citation: Raznichenka, V. D., Shkabrou, A. U., Lazovikava, L. U. (2025). Development of a spectrophotometric approach for assessing pork quality during storage. *Theory and Practice of Meat Processing,* 10(2), 237–246. https://doi.org/10.21323/2414-438X-2024-10-3-237-246

Introduction

Global meat production has more than tripled over the past 50 years and currently amounts to approximately 370 million tons per year [1,2]. With increasing production, meat quality remains a key factor in consumer choice. However, significant quality deterioration and losses occur at all stages, from production to consumption of food products. The share of meat losses worldwide varies from 14 % to 20 % [3,4]. Significant losses occur at various stages before and during slaughter, and quality deterioration occurs throughout the whole food distribution chain [3]. One of the main reasons for this is the insufficient development of a quality control strategy, as well as the limited use of modern analytical methods due to the requirements for the use of traditional approaches. This is due to the lack of adaptation and metrological evaluation of new methods [5].

As noted by the authors [6], traditional methods of meat quality assessment based on physical and chemical analytical approaches retain the status of standard ones, however, they have significant limitations, such as invasiveness, labor intensity and duration [7], which complicates their use in express control systems in production environment [8].

In a critical review by Chen et al. [9], it is shown that in order to overcome the limitations of traditional methods and ensure effective quality control of meat at all stages of production and distribution chain, it is necessary to develop and implement appropriate innovative analytical systems. Such systems should be high-sensitive, compact, integratable into production processes, non-invasive and economically feasible.

An analysis of scientific papers published from 2015 to 2025 on the topic of meat quality and its detection methods showed a shift in emphasis towards non-invasive and high-precision technologies, such as hyperspectral imaging (HSI) [10], Raman spectroscopy [11], ultraviolet (UV) spectrophotometry [12], visible and near infrared (VIS-NIR) spectroscopy [13]. The methods described by the authors allow for multiparameter analysis (water, fat, protein content, freshness) with minimal data processing duration and the ability to integrate into production lines.

According to the study by Ayaz et al. [14], the use of hyperspectral imaging (HSI) to detect meat adulteration demonstrates a fairly high accuracy (94 %), which is significantly higher than most traditional methods. By integrating spectroscopy and visualization, this technology allows for simultaneous acquisition of spectral and spatial data, which significantly expands the capabilities of meat quality and safety assessment. But despite the progress of HSI technology, it has a number of significant disadvantages: a large volume of data, which complicates processing and application in real time; high cost of equipment, which limits widespread implementation; labor-intensive calibration and updating of models, which require significant resources [15].

As shown in a review by Pchelkina et al. [16], Raman spectroscopy allows predicting the quality indicators of meat raw materials with a high degree of reliability and obtaining a large amount of information about the object without its destruction. The method allows to evaluate the sensory indicators, autolytic changes, spoilage, authenticity of raw materials, technological properties, protein structure, fatty acid composition, as well as the differentiation of muscles and tissues [17]. An important advantage of the method is the comparability of the obtained results with the data of traditional analytical methods. However, despite the advantages of this method, there are also some disadvantages, including the complexity of the equipment and data interpretation, as well as limited availability.

The advantages of using visible (VIS) and near infrared (NIR) spectroscopy in the meat industry are thoroughly described in the works by Nechiporenko et al. [18], Wu et al. [19], Tang et al. [20]. The method is successfully used to analyze the composition of muscle tissue, describe the destructive processes occurring during aging, cooling, freezing and storage, as well as for the simultaneous determination of several meat quality parameters, identifying the fact of adulteration, determining the moisture, protein, and fat content, pH, freshness of beef, lamb, pork, chicken and seafood.

Despite the fact that VIS-NIR spectroscopy is a promising tool for monitoring the quality and safety of meat, it requires taking into account the specifics of the samples, numerous physical and chemical experiments before modeling, optimization of models, and has some limitations [21]. Wang et al. noted [22] that for a comprehensive assessment of meat quality, NIRS should be combined with other non-destructive methods to increase its efficiency. The works by Zheng et al. [23] and Cheng et al. [24] emphasize the need for efficient extraction of spectral information, increasing the signal-to-noise ratio, and proper processing of the obtained spectral data to eliminate errors in their interpretation.

Pre-processing of spectral data to improve predictive performance requires the correct choice of appropriate mathematical methods, depending on the objectives [25]. The main goal of pre-processing in spectroscopy is to reduce the influence of scattering and noise in order to isolate the part of the spectrum associated with chemical, physical or biological properties of the studied object. For example, the Savitzky Golay Smoothing Filter (SGSF) method is widely used to eliminate high-frequency noise interference and preserve the peak shape [26]. Cubic spline fitting (CSS) is used to smooth spectra and reduce random noise. The use of first and second derivatives may eliminate the influence of systemic background, such as baseline drift, and increase the resolution of overlapping absorption bands, which allows revealing hidden peaks and improving the identification of chromophores [27]. Moreover, averaging and centering are also common methods of spectral pre-processing.

Modern advances in spectrophotometry, including the use of visible (VIS), near infrared (NIR) and ultraviolet (UV) ranges, as well as integration with chemometric methods, bring new opportunities for analyzing the structure and composition of muscle tissue. However, as the analysis of publications in this area has shown, today there is no common spectral database for meat raw materials, and there are no standardized methods for conducting research and processing the results. Thus, the use of spectroscopic and spectrophotometric methods is a new, promising and relevant area of research in the field of meat quality.

The purpose of this study is to adapt the spectrophotometric method for assessing autolytic changes and monitoring the quality of meat during storage. To achieve this goal, it was proposed to use muscle tissue extracts, since spectroscopy of a piece of meat only evaluates its surface properties, which leads to multiple errors and unreliability of this approach. Therefore, one of the objectives of this work was to determine the optimal extractant for the isolation of protein and non-protein components, suitable for spectrophotometric analysis of meat quality during storage, because sarcoplasmic, myofibrillar and matrix proteins of muscle tissue have different solubility depending on their structure and environmental conditions [28,29].

Objects and methods

The objects of the study were chilled samples of pork longissimus muscle (*Sus scrofa M. longissimus dorsi*) 24 hours after slaughter with a pH value of 5.82 ± 0.20. The meat samples were obtained from various representative half-carcasses of crossbred pork (Yorkshire × Landrace × Duroc) aged 170–180 days, weighing 77–95 kg at Slutsk Meat Processing Plant JSC, Republic of Belarus, and delivered to the laboratory in an isothermal bag within one hour after sampling. The meat was packed in polyethylene bags and stored at a temperature of 2 ± 2 °C for 6 days. Sampling and sample preparation for testing were carried out in accordance with GOST 7269–2015[1] and GOST R 51447–99

[1] GOST 7269–2015 "Meat. Methods of sampling and organoleptic methods of freshness test". Moscow: Standartinform, 2019. Retrieved from https://docs.cntd.ru/document/1200133105 Accessed August 20, 2025 (In Russian)

(ISO 3100–1–91)[2]. Longissimus muscle samples were tested according to the scheme below every day during 6 days of storage.

Preparing aqueous meat extracts

The connective tissue and fat were trimmed, then meat raw material was minced twice in Vitek VT-3624 meat grinder (Star Plus Limited, China) pre-cooled to 4 ± 2 °C with a grate outlet diameter of 2–3 mm. To obtain an aqueous extract, a sample of the minced meat (20.00 ± 0.02 g) was placed in a 250 cm^3 titration flask and extracted with distilled water with a temperature of no higher than 4 ± 2 °C (minced meat to water ratio of 1:5) on SHR-1D laboratory shaker for 30 min. The resulting extract was filtered first through cheesecloth folded in four, and then through a "white ribbon" paper filter with a pore size of 8–12 μm at an ambient temperature of 20 °C.

Preparing NaCl meat extracts

A sample of minced meat (20.00 ± 0.02 g), prepared according to the scheme described above, was placed in a 250 cm^3 titration flask and extracted with a cold (4 ± 2 °C) isotonic sodium chloride solution with NaCl concentration of 0.9 % (minced meat to extractant ratio of 1:5) on SHR-1D laboratory shaker for 30 min. The resulting extract was filtered similarly to aqueous extracts.

Preparing borate buffer meat extracts

A sample of minced meat (20.00 ± 0.02 g) was placed in a 250 cm^3 titration flask and extracted with a borate buffer (sodium tetraborate decahydrate $Na_2B_4O_7 \cdot 10H_2O$) with a concentration of 0.01 mol/l, pH 9.18 and a temperature of no higher than 4 ± 2 °C (minced meat to buffer ratio of 1:5) on SHR-1D laboratory shaker for 30 min. The resulting extract was filtered similarly to aqueous extracts.

Preparing KCl meat extracts

A sample of minced meat (20.00 ± 0.02 g) was placed in a 250 cm^3 titration flask and extracted with a 5 % KCl solution with a temperature no higher than 4 ± 2 °C (minced meat to extractant ratio of 1:5) with constant stirring on SHR-1D laboratory shaker for 30 minutes. The resulting extract was filtered similarly to aqueous extracts.

Registration of absorption spectra

Registration of the absorption spectra of the extracts was carried out on research-grade spectrophotometers, SF-2000 (Zagorsk Optical and Mechanical Plant, Russia) and PE5400VI (Ekokhim, Russia). Extractant solutions were used as comparison solutions (blank solutions). Spectrophotometer operation and preliminary data processing were performed using the included software. Scanning of the absorption spectra of the extracts was carried out in quartz cuvettes with an optical path length of 1 cm and wavelength range of 315–1000 nm, with a scanning step of 5 nm in the optical density measurement mode.

[2] GOST R51447–99 "Meat and meat products. Methods of primary sampling". Moscow: Standartinform, 2018. Retrieved from https://docs.cntd.ru/document/1200028183 Accessed August 19, 2025 (In Russian)

Processing of data obtained

The data obtained as a result of spectrophotometry were averaged using Excel 2019 software (Microsoft, USA) for each sample and presented graphically as a linear diagram or spline.

When processing the spectra in OriginPro 2024 software (OriginLab Corporation, USA), the baseline was calculated using asymmetric least-squares smoothing. The asymmetry factor was taken equal to 0.001. The threshold determining which peaks are considered significant, was taken equal to 0.05. The number of iterations that the method performs to refine the baseline was set equal to 100.

An increase in the absorption spectra resolution was achieved by calculating the second derivative. The smoothing window size was set to 0. Noise filtration during the second derivative analysis was performed using Savitzky Golay Smoothing Filters (SGSF). The points of window used in SGSF method was set to 5. Peak filtration was not applied, and all peaks found were taken into account for further analysis.

The following output data was obtained as a result of the calculations described above:

1) Peak Area;
2) Percent Area;
3) Curve Area;
4) Beginning X;
5) Ending X;
6) Peak Center;
7) Peak Height;
8) FWHM (Full Width at Half Maximum);
9) Peak Centroid;
10) Total area under curve at baseline $Y = 0$.

Histological study

To study the microstructure, 3 × 3 × 3 cm samples were taken from each object of study and fixed in 10 % neutral buffered formalin solution for at least 72 hours at room temperature. For further study, two 1.5 × 1.5 × 0.5 cm pieces with longitudinal and transverse orientation of muscle fibers were taken from each fixed sample. The pieces were washed with cold running water for 4 hours, then compacted in gelatin (AppliChem GMBH, Germany) in ascending concentration (12.5 %, 25 %) using TS-1/20 SPU thermostat (Smolensk SKTB-SPU, Russia) at a temperature of 37 °C for 8 hours in each. Sections 14 μm thick were prepared on Kedee KD-3000 cryostat (Kedee, China) at a temperature of minus 35 °C. Three sections were made from each piece. The obtained sections were mounted on glass (Minimed LLC, Russia), stained with Ehrlich hematoxylin and 1 % aqueous-alcoholic eosin solution (BioVitrum, Russia), and then embedded in glycerin-gelatin.

Histological preparations were studied and photographed with AxioImaiger A1 light microscope (Carl Zeiss, Germany) using AxioCam MRc 5 video camera (Carl Zeiss, Germany) and AxioVision 4.7.1.0 image analysis software (Carl Zeiss, Germany).

Statistical analysis

Statistical analysis of the results was performed using Excel 2019 software (Microsoft, USA). Multiple comparisons between sample groups were performed using OriginPro 2024 software (OriginLab Corporation, USA). The results obtained were considered significant at $p < 0.05$.

Literature data analysis

To select and analyze literature data, taking into account the degree of their relevance, scientific articles, monographs and dissertation abstracts published between 2015 and 2025, available in scientific databases such as Elsevier, PubMed, ResearchGate, Web of Science, Scopus, eLIBRARY.RU, cyberleninka.ru, and CNKI (China National Knowledge Infrastructure) were analyzed.

The search was carried out using the keywords: "meat extract absorption spectra", "myoglobin spectroscopy", "muscle tissue optical properties", "spectrophotometric analysis of meat", "肉类提取物吸收光谱" (absorption spectra of meat extracts), "肉类蛋白质光谱分析" (spectroscopy of meat proteins). The obtained information was processed using systematic approach and logical generalization.

Results and discussion

Spectrophotometric evaluation of extraction methods

As a result of comparative spectrophotometric analysis (Figure 1), it was found that when extracting with different extractants (distilled water, borate buffer, 0.9 % NaCl solution, 5 % KCl solution), the shape and nature of the spectral curves were almost the same in all cases. In the UV–VIS region of the spectrum in the wavelength range of $\lambda_{315–600}$, several of the most intense (major) peaks were observed. In the infrared region (over 700 nm), absorption was significantly reduced, and the spectral curves were flatter.

The main difference between the obtained absorption spectra was the different intensity due to the concentration, chemical nature and physicochemical properties of the extracted substances and extractants [30,31]. The spectra of aqueous extracts were characterized by the lowest integral value of optical density, since distilled water extracts only water-soluble (sarcoplasmic) proteins [32], which are comparatively less numerous than myofibrillar proteins [33,34]. Despite the fact that aqueous extraction is simple and cost-effective, it is limited by the extreme instability of solutions [35] and the isolation of only water-soluble proteins, which may affect the sensitivity of spectrophotometric analysis.

The absorption spectra of buffer extracts had a comparatively higher integrated optical density compared to the spectral profiles of aqueous extracts. This is due to the ability of the borate buffer to extract both sarcoplasmic and myofibrillar proteins, but the completeness of extraction was noticeably lower than that of the KCl and NaCl extracts due to the probable formation of aggregates, which is consistent with the results by Perry et al. [36].

KCl and NaCl extracts demonstrated the highest integrated optical density values compared to aqueous and buffer extracts, providing stable and reproducible results even with small pH fluctuations, since solutions of these salts effectively extract both myofibrillar and sarcoplasmic proteins without pronounced side effects [37], which is consistent with the results by Vasilevskaya et al. [38], Munasinghe et al. [39].

When comparing the shape of the spectra, it was found that aqueous and NaCl extracts had smoother spectral curves with less pronounced (diffuse) peaks, while buffer and KCl extracts were distinguished by clearer and more resolved peaks. The observed differences in the spectra are due to the ability of the extractants used to extract specific substances of muscle tissue (proteins, nucleic acids) and affect their optical properties, which is consistent with the results in [32,36–39] and the Beer-Lambert law.

For a more detailed study of the obtained spectra and an objective choice of the optimal extractant suitable for spectrophotometric analysis of meat quality during storage, a comprehensive processing of the experimental data was carried out. In particular, preliminary processing of the spectra, integration, as well as the search and analysis

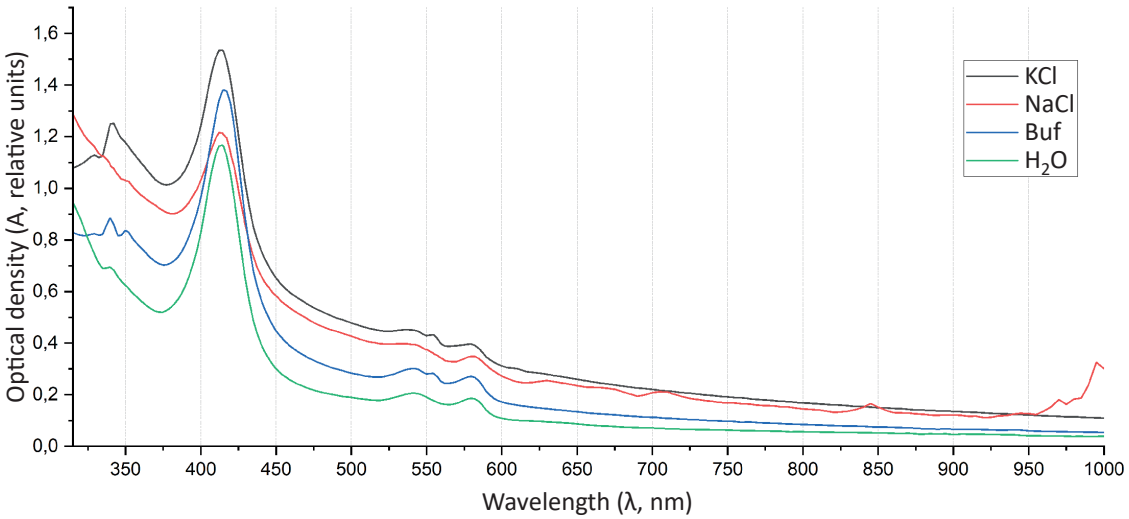

Figure 1. Absorption spectra of pork muscle tissue: (from top to bottom) KCl extract; NaCl extract; borate buffer extract; aqueous extract

of the maxima and minima of absorption in the spectral curves were carried out in accordance with the methods described in [40,41].

Analysis of absorption spectra

When analyzing the absorption spectra, it was taken into account that muscle tissue extracts are multicomponent colloidal systems containing proteins, lipids, and other biologically active compounds. It is known [42] that the main contribution to the absorption spectra in the visible region is made by chromoproteins, such as myoglobin, which amounts 90–95 % of all meat pigments, and hemoglobin. Myoglobin, which contains a heme group with an iron ion (Fe^{2+} or Fe^{3+}) and a porphyrin ring, exhibits typical absorption bands that depend on its oxidation-reduction state.

Deoxymyoglobin demonstrates an absorption maximum at 557 nm, while metmyoglobin demonstrates it at 503 nm. Oxymyoglobin and carboxymyoglobin are characterized by double peaks (doublets): 542/582 nm and 543/581 nm, respectively. The intersection of the spectra of all myoglobin forms at 525 nm (isobestic point) allows to estimate its total concentration in solutions and extracts of fresh meat [43].

An additional contribution to the spectra is made by lipopigments (lipofuscin) [44] and heme breakdown products (bilirubin, biliverdin), which are active in the UV and visible regions [45–47].

A comparative analysis of the spectral profiles of the extracts revealed key differences due to the type of extractant. The most pronounced peaks were observed in KCl and NaCl extracts, which is associated with the high efficiency of extraction of myofibrillar and sarcoplasmic proteins.

In all spectra, regardless of the extraction method, a major peak was observed in the region of 410–415 nm (γ-band), which is characteristic of heme-containing proteins (hemoglobin, myoglobin, cytochromes) and mucopolysaccharides. This peak is associated with $\pi \rightarrow \pi^*$ transitions in the porphyrin ring of heme [48,49] and serves as an indicator of the presence of these compounds in tissues.

In the Q-range of the obtained spectra, α-band (λ_{580}) and β-band (λ_{545}), corresponding to myoglobin [50] were distinguished, as well as some minor bands: $\lambda_{610–615}$, $\lambda_{625–635}$, $\lambda_{640–645}$, $\lambda_{665–670}$.

In the near UV region (330–365 nm), peaks due to $\pi \rightarrow \pi^*$ transitions in unsaturated fatty acids of lipids were identified [51]. The highest intensity and resolution of these peaks in KCl extracts confirmed the high efficiency of this type of extraction (Figure 1).

The spectra of aqueous and buffer extracts demonstrated lower intensity of bands in the Q-range and γ-band compared to KCl and NaCl extracts, which is associated with limited solubilization of proteins [37]. Despite the better resolution of peaks in aqueous and buffer extracts (Table 1), KCl and NaCl extracts provided an optimal ratio of intensity and stability of spectral characteristics.

Based on the data obtained, it was concluded that KCl and NaCl extractions are superior to other methods for spectrophotometric analysis. Absorption maxima in the range from 0.2 to 1.0, minimal distortions of peak geometry, and high reproducibility confirm the suitability of these extraction methods. In turn, KCl extracts demonstrated more pronounced peaks, which makes them preferable for monitoring changes in meat quality during storage and establishing a correlation between spectral characteristics and tissue histostructure.

Spectrophotometric analysis of meat quality during storage

Spectrophotometric analysis of pork KCl extracts during six-day storage revealed consistent changes in key spectral parameters reflecting autolytic processes in muscle tissue. Figure 2 shows averaged absorption spectra demonstrating the preservation of the general shape of the curves with changes in peak intensity and position depending on the storage period.

Analysis of the second derivative of the spectra allowed to isolate and identify 125 unique peaks, including key

Table 1. Results of absorption spectra integration of different extracts

Extracts	Peak center, nm	Peak centroid, nm	FWHM	Peak height	Peak area	Percent area, %	Curve area
KCl	415 ± 1.0	411.3 ± 1.0	30.02 ± 1.05	0.78 ± 0.03	27.05 ± 0.95	61.49 ± 2.15	43.99 ± 1.54
	545 ± 1.0	537.3 ± 1.0	19.15 ± 0.67	0.07 ± 0	1.58 ± 0.06	3.58 ± 0.13	
	555 ± 1.0	556.8 ± 1.0	10.00 ± 0.35	0.07 ± 0	0.87 ± 0.03	1.98 ± 0.07	
	580 ± 1.0	579.1 ± 1.0	25.00 ± 0.88	0.08 ± 0	1.7 ± 0.06	3.87 ± 0.14	
NaCl	415 ± 1.0	411.9 ± 1.0	28.96 ± 1.01	0.50 ± 0.02	16.47 ± 0.58	45.24 ± 1.58	36.41 ± 1.27
	545 ± 1.0	538.5 ± 1.0	38.02 ± 1.33	0.07 ± 0	2.88 ± 0.1	7.92 ± 0.28	
	580 ± 1.0	584.0 ± 1.0	30.15 ± 1.06	0.08 ± 0	2.25 ± 0.08	6.17 ± 0.22	
$Na_2B_4O_7 \cdot 10H_2O$	415 ± 1.0	413.7 ± 1.0	28.10 ± 0.98	0.86 ± 0.03	28.13 ± 0.98	66.59 ± 2.33	42.25 ± 1.48
	545 ± 1.0	536.3 ± 1.0	18.89 ± 0.66	0.1 ± 0.01	2.28 ± 0.08	5.40 ± 0.19	
	555 ± 1.0	554.8 ± 1.0	5.00 ± 0.18	0.09 ± 0.01	0.85 ± 0.03	2.01 ± 0.07	
	580 ± 1.0	578.2 ± 1.0	30.85 ± 1.08	0.11 ± 0.01	2.96 ± 0.1	7.00 ± 0.24	
H_2O	415 ± 1.0	413.0 ± 1.0	27.92 ± 0.98	0.78 ± 0.03	24.15 ± 0.85	61.83 ± 2.16	39.06 ± 1.37
	545 ± 1.0	539.0 ± 1.0	31.52 ± 1.1	0.09 ± 0.01	3.11 ± 0.11	7.95 ± 0.28	
	580 ± 1.0	581.1 ± 1.0	32.16 ± 1.13	0.1 ± 0.01	3.08 ± 0.11	7.89 ± 0.28	

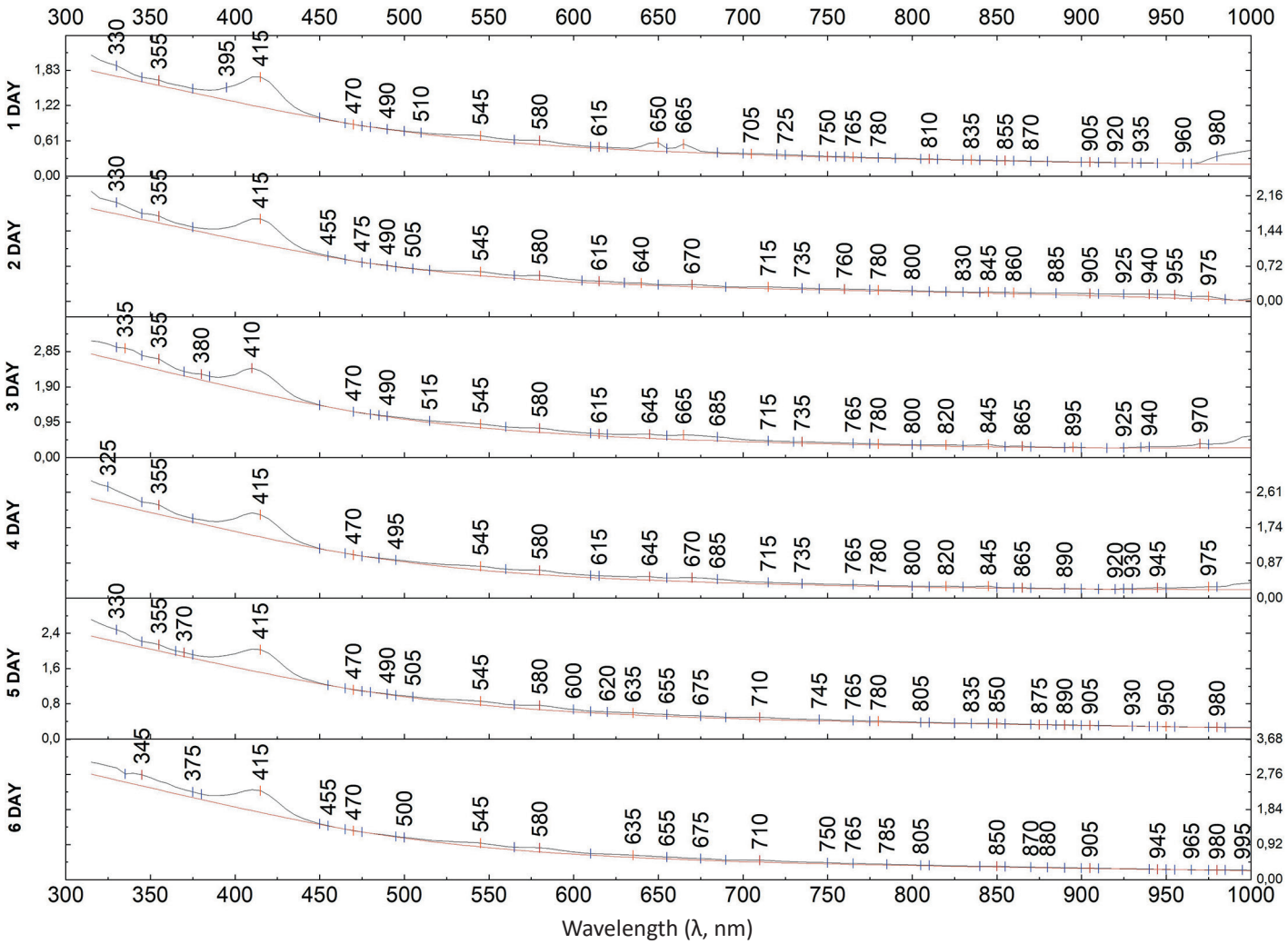

Figure 2. Average absorption spectra of pork muscle tissue KCl extracts at different storage periods

maxima: $\lambda_{325–335}$, λ_{355}, $\lambda_{410–415}$, λ_{545}, λ_{580}, $\lambda_{610–620}$, $\lambda_{635–650}$ (Table 2). The use of the Blackman-Tukey correlogram method in combination with the Tukey HSD test for multiple comparisons between sample groups confirmed the statistical significance ($p < 0.05$) of the differences in the intensity of these peaks between sample groups formed by storage periods.

Minor peaks at $\lambda_{325–335}$ and λ_{355} showed simultaneous dynamics with histological changes in muscle tissue (Figure 3). In the first four days, their height, area and percent area increased, correlating with muscle fiber relaxation and restoration of transverse striation. By the sixth day, the peaks completely disappeared, which corresponded to the development of the aging stage and the onset of destructive processes.

FWHM of peak at $\lambda_{325–335}$ remained stable, while for peak at λ_{355}, narrowing was observed. The hypsochromic shift of peak centroid at λ_{355} by the fifth day (with an unchanged position of the peak center) indicated structural changes in the extracted components associated with lipid oxidation [51,52] and a decrease in NADH/NADPH level [53,54].

According to [54], NADH level decreases statistically significantly ($p < 0.05$) with increasing of meat storage period. This is due to the depletion of metabolites involved in the restoration of NADH, such as fumaric acid, creatinine and fructose, which also decrease over time. For NADPH, there is little direct data on post-slaughter changes in meat, however, given its role in biochemical reactions, it may be assumed that its amount also decreases, since metabolic processes in muscle tissue cease after slaughter. The study [55] notes that during meat storage, there is a change in the oxidation-reduction balance, which may lead to a decrease in the NADPH level, but specific measurements are not presented.

A strong correlation ($r = 0.91$) between the change in peak area at λ_{355} (including its percent area) and the dynamics of muscle fiber diameter indicated the influence of autolytic processes in muscle tissue on the spectral properties of the extracts.

Thus, changes in the indicated values of minor peaks at $\lambda_{325–335}$ and λ_{355} reflect biochemical transformations of extracted components of muscle tissue.

The peak of the γ-band at $\lambda_{410–415}$, associated with heme-containing proteins and mucopolysaccharides [48,49], demonstrated an increase in area up to the third day (19.17 ± 0.64 arbitrary unit) with subsequent stabilization. The hypsochromic shift of peak centroid (4.13 ± 1.24 nm) and the change in FWHM (up to $31.95 \pm .57$ on the sixth day) reflected the degradation of glycosaminoglycans and proteins.

Table 2. Results of absorption spectra integration of chilled pork KCl extracts at different storage periods

Peak (λ, nm)	Days	Peak area	Percent area, %	Curve area	FWHM	Peak height	Peak center, nm	Peak centroid, nm
$\lambda_{325–335}$	1	1,81 ± 0,05	4,26 ± 0,13	42,46 ± 1,27	10 ± 0,31	0,18 ± 0,01	330 ± 1,00	336,32 ± 1,00
	2	2,63 ± 0,08	5,7 ± 0,17	46,24 ± 1,39	10 ± 0,30	0,23 ± 0,01	330 ± 1,00	336,66 ± 1,00
	3	5,27 ± 0,16	7,65 ± 0,23	68,92 ± 2,07	10 ± 0,31	0,37 ± 0,01	335 ± 1,00	337,33 ± 1,00
	4	6,03 ± 0,18	10,24 ± 0,31	58,83 ± 1,76	15 ± 0,45	0,4 ± 0,01	325 ± 1,00	334,02 ± 1,00
	5	3,06 ± 0,09	6,86 ± 0,21	44,63 ± 1,34	10 ± 0,33	0,28 ± 0,01	330 ± 1,00	336,52 ± 1,00
	6	—	—	—	—	—	—	—
λ_{355}	1	2,4 ± 0,07	5,65 ± 0,17	42,46 ± 1,27	25 ± 0,75	0,09 ± 0,01	355 ± 1,00	359,55 ± 1,00
	2	3,16 ± 0,09	6,83 ± 0,2	46,24 ± 1,39	23,94 ± 0,72	0,14 ± 0,01	355 ± 1,00	357,72 ± 1,00
	3	5,75 ± 0,17	8,35 ± 0,25	68,92 ± 2,07	19,53 ± 0,59	0,3 ± 0,01	355 ± 1,00	355,57 ± 1,00
	4	5,02 ± 0,15	8,53 ± 0,26	58,83 ± 1,76	19,63 ± 0,59	0,24 ± 0,01	355 ± 1,00	357,28 ± 1,00
	5	2,56 ± 0,08	5,73 ± 0,17	44,63 ± 1,34	15 ± 0,45	0,15 ± 0,01	355 ± 1,00	354,24 ± 1,00
	6	—	—	—	—	—	—	—
$\lambda_{410–415}$	1	15,14 ± 0,45	35,66 ± 1,07	42,46 ± 1,27	30,23 ± 0,91	0,52 ± 0,02	415 ± 1,00	415,59 ± 1,00
	2	17,52 ± 0,53	37,88 ± 1,14	46,24 ± 1,39	29,56 ± 0,89	0,52 ± 0,02	415 ± 1,00	412,61 ± 1,00
	3	19,71 ± 0,59	28,59 ± 0,86	68,92 ± 2,07	29,12 ± 0,87	0,63 ± 0,02	410 ± 1,00	412,5 ± 1,00
	4	18,89 ± 0,57	32,11 ± 0,96	58,83 ± 1,76	30,35 ± 0,91	0,55 ± 0,02	415 ± 1,00	410,92 ± 1,00
	5	18,25 ± 0,55	40,9 ± 1,23	44,63 ± 1,34	31,69 ± 0,95	0,52 ± 0,02	415 ± 1,00	411,47 ± 1,00
	6	19,81 ± 0,59	37,03 ± 1,11	53,51 ± 1,61	31,95 ± 0,96	0,57 ± 0,02	415 ± 1,00	411,46 ± 1,00
λ_{545}	1	2,69 ± 0,08	6,33 ± 0,19	42,46 ± 1,27	35,47 ± 1,06	0,07 ± 0,01	545 ± 1,00	541,39 ± 1,00
	2	2,94 ± 0,09	6,35 ± 0,19	46,24 ± 1,39	32,84 ± 0,99	0,08 ± 0,01	545 ± 1,00	543,56 ± 1,00
	3	3,55 ± 0,11	5,15 ± 0,15	68,92 ± 2,07	35,5 ± 1,06	0,1 ± 0,01	545 ± 1,00	539,77 ± 1,00
	4	3,85 ± 0,12	6,55 ± 0,2	58,83 ± 1,76	34,91 ± 1,05	0,09 ± 0,01	545 ± 1,00	534,6 ± 1,00
	5	3,54 ± 0,11	7,93 ± 0,24	44,63 ± 1,34	37,79 ± 1,13	0,09 ± 0,01	545 ± 1,00	540,04 ± 1,00
	6	4,08 ± 0,12	7,62 ± 0,23	53,51 ± 1,61	37,72 ± 1,13	0,1 ± 0,01	545 ± 1,00	538,78 ± 1,00
λ_{580}	1	2,26 ± 0,07	5,33 ± 0,16	42,46 ± 1,27	32,11 ± 0,96	0,07 ± 0,01	580 ± 1,00	584,14 ± 1,00
	2	2,74 ± 0,08	5,93 ± 0,18	46,24 ± 1,39	35 ± 1,05	0,09 ± 0,01	580 ± 1,00	583,38 ± 1,00
	3	4,32 ± 0,13	6,27 ± 0,19	68,92 ± 2,07	45 ± 1,35	0,11 ± 0,01	580 ± 1,00	583,55 ± 1,00
	4	4,01 ± 0,12	6,81 ± 0,2	58,83 ± 1,76	45 ± 1,35	0,11 ± 0,01	580 ± 1,00	583,37 ± 1,00
	5	2,68 ± 0,08	6,01 ± 0,18	44,63 ± 1,34	30 ± 0,9	0,1 ± 0,01	580 ± 1,00	582 ± 1,00
	6	3,52 ± 0,11	6,57 ± 0,2	53,51 ± 1,61	36,19 ± 1,09	0,11 ± 0,01	580 ± 1,00	585,19 ± 1,00
$\lambda_{610–620}$	1	0,24 ± 0,01	0,57 ± 0,02	42,46 ± 1,27	5 ± 0,15	0,02 ± 0	615 ± 1,00	615,05 ± 1,00
	2	1,05 ± 0,03	2,27 ± 0,07	46,24 ± 1,39	20 ± 0,6	0,04 ± 0	615 ± 1,00	617,24 ± 1,00
	3	0,61 ± 0,02	0,88 ± 0,03	68,92 ± 2,07	5 ± 0,15	0,06 ± 0	615 ± 1,00	615 ± 1,00
	4	0,29 ± 0,01	0,49 ± 0,01	58,83 ± 1,76	610 ± 18,3	0,06 ± 0	615 ± 1,00	612,51 ± 1,00
	5	0,39 ± 0,01	0,87 ± 0,03	44,63 ± 1,34	610 ± 18,3	0,04 ± 0	620 ± 1,00	615,07 ± 1,00
	6	—	—	—	—	—	—	—
$\lambda_{635–650}$	1	2,37 ± 0,07	5,59 ± 0,17	42,46 ± 1,27	10,04 ± 0,3	0,15 ± 0	650 ± 1,00	643,19 ± 1,00
	2	0,67 ± 0,02	1,44 ± 0,04	46,24 ± 1,39	15 ± 0,45	0,04 ± 0	640 ± 1,00	639,31 ± 1,00
	3	3,05 ± 0,09	4,42 ± 0,13	68,92 ± 2,07	30 ± 0,9	0,11 ± 0	645 ± 1,00	639,25 ± 1,00
	4	2,74 ± 0,08	4,66 ± 0,14	58,83 ± 1,76	35 ± 1,05	0,09 ± 0	645 ± 1,00	636,41 ± 1,00
	5	1,51 ± 0,05	3,39 ± 0,1	44,63 ± 1,34	30 ± 0,9	0,05 ± 0	635 ± 1,00	637,44 ± 1,00
	6	2,35 ± 0,07	4,4 ± 0,13	53,51 ± 1,61	40 ± 1,2	0,06 ± 0	635 ± 1,00	632,97 ± 1,00

In the first three days, β-band (λ_{545}) and α-band (λ_{580}) in the Q-range showed an increase in area, with the latter being characterized by a significant ($p < 0.05$) change in geometry (increase in FWHM and height).

It was found that the indicated processes on the α-, β- and γ-bands occurred simultaneously with histostructural changes in muscle tissue and the onset of various autolysis stages.

As is the case of the minor peak at λ_{355}, similar dynamics were observed in $\lambda_{610–620}$ region, where an increase in peak area occurred on the first day, followed by a decrease and complete disappearance by day 6. In turn, a bathochromic shift of peak center by 5 nm was detected in the indicated wavelength range while maintaining the position of peak centroid.

A fourfold increase in FWHM and a hypochromic shift of peak centroid (10.22 ± 1.92 nm) in $\lambda_{635–650}$ region indicated the accumulation of lipid oxidation products, which is consistent with [52].

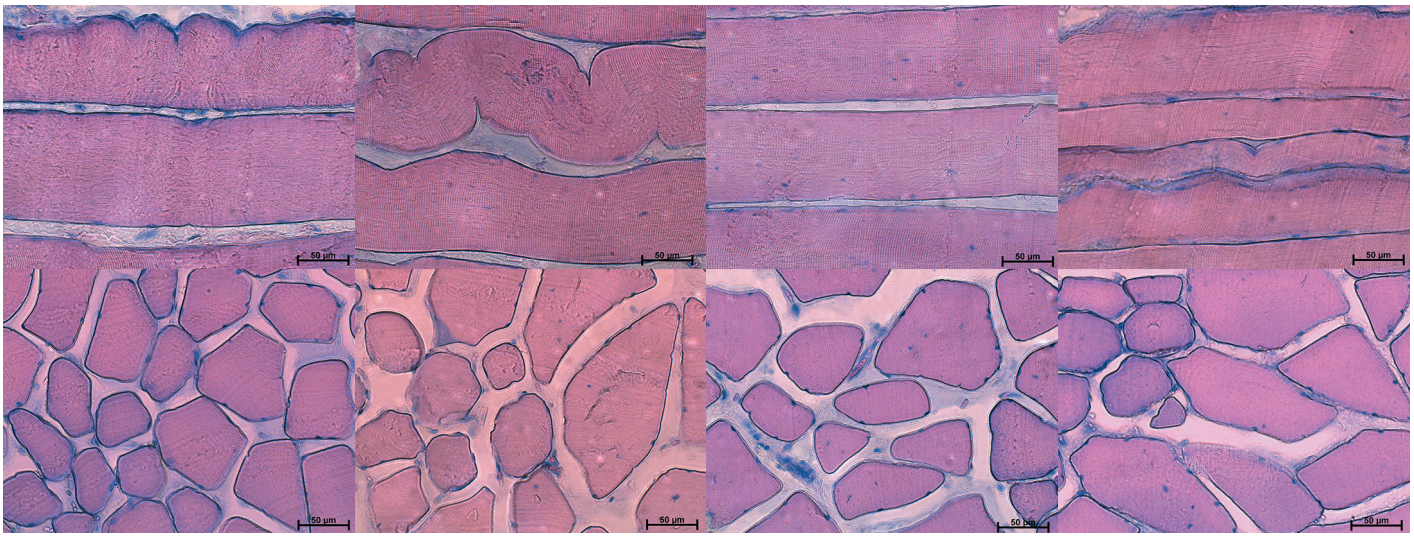

(a) (b) (c) (d)

Figure 3. Histostructure of *Sus scrofa M. longissimus dorsi* muscle tissue on the first (a), third (b), fifth (c) and sixth (d) days of storage (40× magnification)

A change in the integral parameters of the peaks indicates an increase or decrease in the concentration of certain substances in meat during storage. In turn, a change in the geometry (FWHM, peak center and peak centroid) of the peaks indicates structural and chemical changes in these substances. The results of the study prove that, depending on the degree of autolytic changes in muscle tissue, characteristic changes in the intensity and geometry of the above peaks occur. The use of KCl extraction in combination with data preprocessing made it possible to establish clear patterns consistent with histological studies (Figure 3).

The dynamics of minor peaks at $\lambda_{325–335}$, λ_{355} and γ-band at $\lambda_{410–415}$ reflected the stages of rigor mortis and meat aging simultaneously with histological transformations (restoration of transverse striation, relaxation and change in the diameter of muscle fibers). Changes in the Q-range (λ_{545}, λ_{580}) and $\lambda_{635–650}$ region confirmed the accumulation of oxidation products, which allows using these parameters as markers of oxidative spoilage. This confirms the potential of the method for objective assessment of meat quality, predicting shelf life and monitoring structural and chemical changes in muscle tissue.

Conclusion

The study confirmed the effectiveness of spectrophotometric analysis of pork KCl extracts for monitoring meat quality during storage. It was found that KCl extraction provides high solubilization of myofibrillar and sarcoplasmic proteins, forming stable spectral profiles with clearly defined peaks. Key spectral parameters (peak area, FWHM, peak centroid) demonstrated statistically significant correlation ($p < 0.05$) with autolytic processes in muscle tissue, including physicochemical and histostructural changes.

The obtained data confirm that the spectral characteristics of muscle tissue KCl extracts, reflecting the dynamics of pigments (myoglobin, NADH), structural proteins and other compounds interaction, serve as reliable markers of autolytic transformations. Quantitative analysis of the integral parameters of key peaks at $\lambda_{325–335}$, λ_{355}, $\lambda_{410–415}$, λ_{545}, λ_{580}, $\lambda_{610–620}$, $\lambda_{635–650}$ allows objectifying the assessment of the autolysis degree. Integral analysis of spectral characteristics allows not only to assess the autolysis degree, but also to identify specific patterns characteristic of meat at different storage periods.

The ability to monitor changes occurring in pork muscle tissue during storage using spectrophotometry emphasizes its value as a tool for assessing meat quality and brings opportunities for the development of fast and reliable methods for quality control of meat products. However, to fully realize the potential of the method, further research is needed to standardize the analysis conditions and expand the spectral characteristics databases.

REFERENCES

1. Ritchie, H., Rosado, P., Roser, M. (2019). Meat and Dairy Production. Retrieved from: https://ourworldindata.org/meat-production Accessed 14 April 2025
2. FAO. (2024). Meat market review. Emerging trends and outlook in 2024. Rome, FAO, 2024.
3. FAO. (2022). Voluntary code of conduct for food loss and waste reduction. Rome, FAO, 2022. https://doi.org/10.4060/cb9433en
4. Aldamatov, N. E., Bredikhin, S. A. (2024). Production of raw materials of animal origin in the world and in Russia. *Scientific Journal of the Far Eastern State Technical Fisheries University*, 70(4), 8–19. https://doi.org/10.48612/dalrybvtuz/2024-70-01 (In Russian)
5. Yushina, Yu. K., Kulikovskii, A. V. Stanovova, I.A. (2016). Unification control methods of the qualitative characteristics of meat and meat products. *Vsyo o Myase*, 4, 18–21. (In Russian)
6. Anagnostou, G., Ferragina, A., Crofton, E. C., Frias Celayeta, J. M., Hamill, R. M. (2025). The development of optical sensing techniques as digital tools to predict the sensory quality of red meat: A review. *Applied Sciences*, 15(4), Article 1719. https://doi.org/10.3390/app15041719
7. Elangovan, P., Dhurairajan, V., Nath, M. K., Yogarajah, P., Condell, J. (2024). A novel approach for meat quality assessment using an ensemble of compact convolutional neural

networks. *Applied Sciences*, 14(14), Article 5979. https://doi.org/10.3390/app14145979
8. Shi, Y., Wang, X., Borhan, M. S., Young, J., Newman, D., Berg, E. et al. (2021). A review on meat quality evaluation methods based on non-destructive computer vision and artificial intelligence technologies. *Food Science of Animal Resources*, 41(4), 563–588. https://doi.org/10.5851/kosfa.2021.e25
9. Chen, J., Zhang, J., Wang, N., Xiao, B., Sun, X., Li, J. et al. (2024). Critical review and recent advances of emerging real-time and non-destructive strategies for meat spoilage monitoring. *Food Chemistry*, 445, Article 138755. https://doi.org/10.1016/j.foodchem.2024.138755
10. Jia, W., van Ruth, S., Scollan, N., Koidis, A. (2022). Hyperspectral Imaging (HSI) for meat quality evaluation across the supply chain: Current and future trends. *Current Research in Food Science*, 5, 1017–1027. https://doi.org/10.1016/j.crfs.2022.05.016
11. Qu, C., Li, Y., Du, S., Geng, Y., Su, M., Liu, H. (2022). Raman spectroscopy for rapid fingerprint analysis of meat quality and security: Principles, progress and prospects. *Food Research International*, 161, Article 111805. https://doi.org/10.1016/j.foodres.2022.111805
12. Power, A. C., Chapman, J., Chandra, S., Cozzolino, D. (2019). Ultraviolet-visible spectroscopy for food quality analysis. Chapter in a book: Evaluation Technologies for Food Quality. Duxford, United Kingdom: Woodhead Publishing, 2019. https://doi.org/10.1016/B978-0-12-814217-2.00006-8
13. Peyvasteh, M., Popov, A., Bykov, A., Meglinski, I. (2020). Meat freshness revealed by visible to near-infrared spectroscopy and principal component analysis. *Journal of Physics Communications*, 4(9), Article 095011. https://doi.org/10.1088/2399-6528/abb322
14. Ayaz, H., Ahmad, M., Mazzara, M., Sohaib, A. (2020). Hyperspectral imaging for minced meat classification using nonlinear deep features. *Applied Sciences*, 10(21), Article 7783. https://doi.org/10.3390/app10217783
15. Wang, W., Peng, Y. (2018). Hyperspectral imaging for assessing quality and safety of meat. Chapter in a book: Hyperspectral Imaging in Agriculture, Food and Environment. IntechOpen, 2018. https://doi.org/10.5772/intechopen.74371
16. Pchelkina, V. A., Chernukha, I. M., Fedulova, L. V., Ilyin, N. A. (2022). Raman spectroscopic techniques for meat analysis: A review. *Theory and Practice of Meat Processing*, 7(2), 97–111. https://doi.org/10.21323/2414-438X-2022-7-2-97-111
17. Shoko, P. T., Blanch, E. W., Torley, P. J., Pillidge, C. (2024). Raman spectroscopy for the differentiation of muscles and tissues in meat using chicken as a model system. *Journal of Raman Spectroscopy*, 55(11), 1146–1155. https://doi.org/10.1002/jrs.6725
18. Nechiporenko, A. P., Orehova, S. M., Plotnikova, L. V., Plotnikov, P. P. (2019). Diffuse-reflection electron spectroscopy in the study of muscle tissue of wild and domestic animals. *Proceedings of Universities. Applied Chemistry and Biotechnology*, 9(3), 489–499. https://doi.org/10.21285/2227-2925-2019-9-3-489-499 (In Russian)
19. Wu, X., Liang, X., Wang, Y., Wu, B., Sun, J. (2022). Non-destructive techniques for the analysis and evaluation of meat quality and safety: A review. *Foods*, 11(22), Article 3713. https://doi.org/10.3390/foods11223713
20. Tang, X., Xie, L., Liu, S., Chen, Z., Rao, L., Chen, L. et al. (2022). Extensive evaluation of prediction performance for 15 pork quality traits using large scale VIS/NIRS data. *Meat Science*, 192, Article 108902. https://doi.org/10.1016/j.meatsci.2022.108902
21. Leder, P. J. S., Porcu, O. M. (2018). The importance of UV–VIS spectroscopy: Application in food products characterization. *Scholarly Journal of Food Nutrition*, 1(3), 59–62. https://doi.org/10.32474/SJFN.2018.01.000111
22. Wang, D., Luan, Y., Wang, X., Jia, W. (2024). Progress in non-destructive analysis of meat quality by near-infrared spectroscopy. *Meat Research*, 38(5), 61–70. https://doi.org/10.7506/rlyj1001-8123-20240513-118
23. Zheng, X., Chen, L., Li, X., Zhang, D. (2023). Non-destructive detection of meat quality based on multiple spectral dimension reduction methods by near-infrared spectroscopy. *Foods*, 12(2), Article 300. https://doi.org/10.3390/foods12020300
24. Cheng, L.J., Liu, G.S., He, J.G. (2021). Development of a novel quantitative function between spectral value and metmyoglobin content in Tan mutton. *Food Chemistry*, 342, Article 128351. https://doi.org/10.1016/j.foodchem.2020.128351
25. Barra, I., Briak, H., Kebede, F. (2022). The application of statistical preprocessing on spectral data does not always guarantee the improvement of the predictive quality of multivariate models: Case of soil spectroscopy applied to Moroccan soils. *Vibrational Spectroscopy*, 121, Article 103409. https://doi.org/10.1016/j.vibspec.2022.103409
26. Tsagkaris, A. S., Bechynska, K., Ntakoulas, D. D., Pasias, I. N., Weller, P., Proestos, C. et al. (2023). Investigating the impact of spectral data pre-processing to assess honey botanical origin through Fourier transform infrared spectroscopy (FTIR). *Journal of Food Composition and Analysis*, 119, Article 105276. https://doi.org/10.1016/j.jfca.2023.105276
27. Lavrinenko, I. A., Vashanov, G. A., Ruban, M. K. (2013). Analysis of the contribution of chromophores in side groups of amino acids to the absorption spectrum of hemoglobin. *Journal of Applied Spectroscopy*, 80(6), 899–904. https://doi.org/10.1007/s10812-014-9862-4
28. Feng, Y.-H., Zhang, S. -S., Sun, B.-Z., Xie, P., Wen, K.-X., Xu, C.-C. (2020). Changes in physical meat traits, protein solubility, and the microstructure of different beef muscles during post-mortem aging. *Foods*, 9(6), Article 806. https://doi.org/10.3390/foods9060806
29. Qiu, Z., Shi, Y., Zheng, Y., Shi, W., Zhang, L., Yin, M. et al. (2025). Comparison of in vitro digestive characteristics of proteins from different sources in simulated elderly gastrointestinal conditions. *Food Chemistry*, 463(3), Article 141299. https://doi.org/10.1016/j.foodchem.2024.141299
30. Chen, K., Zhang, Q., Yang, S., Zhang, S., Chen, G. (2024). Comparative study on the impact of different extraction technologies on structural characteristics, physicochemical properties, and biological activities of polysaccharides from seedless chestnut rose (*Rosa sterilis*) fruit. *Foods*, 13(5), Article 772. https://doi.org/10.3390/foods13050772
31. Al-Behadili, W. K. H., Jawad, Y. M., Whaab, W. S. A. (2023). Effect of solvent on intensity of absorption and fluorescence of Eosin Y Dye and spectral properties of Eosin Y Dye. *Journal of Medicinal and Chemical Sciences*, 6(2), 322–334. https://doi.org/10.26655/JMCHEMSCI.2023.2.13
32. Zaukuu, J.-L. Z., Gillay, Z., Kovacs, Z. (2021). Standardized extraction techniques for meat analysis with the electronic tongue: A case study of poultry and red meat adulteration. *Sensors*, 21(2), Article 481. https://doi.org/10.3390/s21020481
33. Nechiporenko, A. P., Orekhova, S. M., Sitnikova, V. E., Gromova, D. A., Bushueva, A. V., Uspenskaya, M. V. (2021). Fourier spectroscopy of sarcoplasmic, myofibrillar, and connective tissue proteins of pork muscle tissue. *Processes and Food Production Equipment*, 1, 3–14. https://doi.org/10.17586/2310-1164-2021-14-1-3-14 (In Russian)
34. Haque, Md. A., Timilsena, Y. P., Adhikari, B. (2016). Food proteins, structure, and function. Chapter in a book: Reference Module in Food Science. Elsevier, 2016. https://doi.org/10.1016/B978-0-08-100596-5.03057-2
35. Khismatullina, Z.N. (2013). Methods for fractionating a protein mixture into individual proteins. *Herald of Technological University,* 16(21), 212–217. (In Russian)
36. Perry, S. V., Corsi, A. (1958). Extraction of proteins other than myosin from the isolated rabbit myofibril. *Biochemical Journal*, 68(1), 5–12. https://doi.org/10.1042/bj0680005

37. Jiao, X., Li, X., Zhang, N., Yan, B., Huang, J., Zhao, J. (2024). Solubilization of fish myofibrillar proteins in NaCl and KCl solutions: A DIA-based proteomics analysis. *Food Chemistry*, 445, Article 138662. https://doi.org/10.1016/j.foodchem.2024.138662
38. Vasilevskaya, E. R., Aryuzina, M. A., Vetrova, E. S. (2021). Saline extraction as a method of obtaining a mixture of biologically active com pounds of protein nature from a porcine pancreas. *Food Systems*, 4(2), 97–105. https://doi.org/10.21323/2618-9771-2020-4-2-97-105 (In Russian)
39. Munasinghe, D. M. S., Sakai, T. (2004). Sodium chloride as a preferred protein extractant for pork lean meat. *Meat Science*, 67(4), 697–703. https://doi.org/10.1016/j.meatsci.2004.02.001
40. Rinnan, A., Norgaard, L., van den Berg, F., Thygesen, J., Bro, R., Engelsen, S. B. (2009). Data pre-processing. Chapter in a book: Comprehensive Chemometrics: Chemical and Biochemical Data Analysis. Academic Press, 2009. https://doi.org/10.1016/B978-0-12-374136-3.00002-X
41. Czarnecki, M. A. (2015). Resolution enhancement in second-derivative spectra. *Applied Spectroscopy*, 69(1), 67–74. https://doi.org/10.1366/14-07568
42. Ramanathan, R., Suman, S. P., Faustman, C. (2020). Biomolecular interactions governing fresh meat color in post-mortem skeletal muscle: A review. *Journal of Agricultural and Food Chemistry*, 68(46), 12779–12787. https://doi.org/10.1021/acs.jafc.9b08098
43. Shkabrov, O. V., Reznichenko, V. D., Chernukha, I. M., Bolashenko, T. N., Lazovikova, L. V. (2023). Mechanics of meat color formation and methods of its registration. *VESTNIK BGUT: Scientific and Methodical Journal*, 2(35), 44–63. (In Russian)
44. Hasegawa, Y., Kawasaki, T., Maeda, N., Yamada, M., Takahashi, N., Watanabe, T. et al. (2021). Accumulation of lipofuscin in broiler chicken with wooden breast. *Animal Science Journal*, 92(1), Article e13517. https://doi.org/10.1111/asj.13517
45. Ahmmed, E., Mondal, A., Saha, N.C., Dhara, K., Chattopadhyay, P. (2021). A deoxygenation-switch-based red-emitting fluorogenic light-up probe for the detection of highly toxic free bilirubin in human blood serum. *Analytical Methods*, 13(46), 5651–5659. https://doi.org/10.1039/d1ay01717a
46. Santacruz-Perez, C., Tonolli, P. N., Ravagnani, F. G., Baptista, M. S. (2018). Photochemistry of lipofuscin and the interplay of uva and visible light in skin photosensitivity. Chapter in a book: Photochemistry and Photophysics — Fundamentals to Applications. London, UK: IntechOpen, 2018. https://doi.org/10.5772/intechopen.76641
47. McEwen, M., Reynolds, K. (2006). Noninvasive detection of bilirubin using pulsatile absorption. *Australasian Physical and Engineering Sciences in Medicine*, 29(1), 78–83.
48. Wajda, A., Dybas, J., Kachamakova-Trojanowska, N., Pacia, M.Z., Wilkosz, N., Bułat, K. et al. (2024). Raman imaging unveils heme uptake in endothelial cells. *Scientific Reports*, 14(1), Article 20684. https://doi.org/10.1038/s41598-024-71600-2
49. Schweitzer-Stenner, R. (2014). Cytochrome c: A multifunctional protein combining conformational rigidity with flexibility. *New Journal of Science*, 2014, Article 484538. https://doi.org/10.1155/2014/484538
50. Espitia-Almeida, F., Diaz-Uribe, C., Vallejo, W., Gómez-Camargo, D., Bohórquez, A.R.R., CLinares-Flores, C. (2021). Photophysical study and *in vitro* approach against leishmania panamensis of dicloro-5,10,15,20-Tetrakis(4-bromophenyl)porphyrinato Sn(IV). *F1000 Research*, 10, Article 379. https://doi.org/10.12688/f1000research.52433.3
51. Orehova, S., Nechiporenko, U., Vasileva, I., Nechiporenko, A. (2011). *Electronic spectrum of pork and beef muscle tissue surface samples subjected to electron-radiation processing*. Processing 6th Baltic Conference on Food Science and Technology: Innovations for Food Science and Production (FOODBALT-2011). Latvia, Jelgava, 2011.
52. Domínguez, R., Pateiro, M., Gagaoua, M., Barba, F. J., Zhang, W., Lorenzo, J. M. (2019). A Comprehensive review on lipid oxidation in meat and meat products. *Antioxidants*, 8(10), Article 429. https://doi.org/10.3390/antiox8100429
53. De Ruyck, J., Famerée, M., Wouters, J., Perpète, E. A., Preat, J., Jacquemin, D. (2007). Towards the understanding of the absorption spectra of NAD(P)H/NAD(P)+ as a common indicator of dehydrogenase enzymatic activity. *Chemical Physics Letters*, 450(1–3), 119–122. https://doi.org/10.1016/j.cplett.2007.10.092
54. Mitacek, R. M., Ke, Y., Prenni, J. E., Jadeja, R., VanOverbeke, D.L., Mafi, G.G. et al. (2019). Mitochondrial degeneration, depletion of NADH, and oxidative stress decrease color stability of wet-aged beef longissimus steaks. *Journal of Food Science*, 84(1), 38–50. https://doi.org/10.1111/1750-3841.14396
55. Ramanathan, R., Mafi, G. G., Yoder, L., Perry, M., Pfeiffer, M., VanOverbeke, D. L. et al. (2020). Biochemical changes of postmortem meat during the aging process and strategies to improve the meat quality. Chapter in a book: Meat Quality Analysis. Academic Press, 2020. https://doi.org/10.1016/b978-0-12-819233-7.00005-7

AUTHOR INFORMATION

Viktar D. Raznichenka, Engineer-Technologist, Department of the Chief Technologist, Slutsk Meat Processing Plant JSC, 18, Tutarinov str., Slutsk, Minsk region, 223610, Republic of Belarus. E-mail: rotcivetec@gmail.com
ORCID: http://orcid.org/0000-0002-1537-8482
* corresponding author

Aleh U. Shkabrou, Candidate of Technical Sciences, Docent, Head of the Department of Meat and Dairy Products Technologies, Ministry of Agriculture and Food of the Republic of Belarus, Republic of Belarus. 15, Kirov str., Minsk, 220030, Republic of Belarus. E-mail: olegshk@tut.by
ORCID: http://orcid.org/0000-0002-7188-2237

Lyubou U. Lazovikava, Candidate of Technical Sciences, Docent, Docent, Department of Technology of Public Catering and Meat Products, Belarusian State University of Food and Chemical Technologies. 3, Shmidt Avenue, Mogilev, 212027, Republic of Belarus. E-mail: lyu-azarova@ yandex.by
ORCID: http://orcid.org/0009-0002-7980-9103

All authors bear equal responsibility for the work and presented data.

All authors made an equal contribution to the work.

The authors were equally involved in writing the manuscript and bear the equal responsibility for plagiarism.

The authors declare no conflict of interest.